SLAC-PUB-17119

# AN UNAVOIDABLE TRAPPED MODE IN THE INTERACTION REGION OF COLLIDING BEAMS

Alexander Novokhatski†, Michael Sullivan, SLAC National Accelerator Laboratory, Menlo Park, CA 94025, USA
Eleonora Belli, Miguel Gil Costa and Roberto Kersevan
CERN, 1211 Geneva 23, Switzerland

*Abstract*

We discuss the nature of the electromagnetic fields excited by the beams in the beam pipe of an interaction region. In trying to find an optimum geometry for this region with a minimum of electromagnetic wave excitation, we have discovered one mode, which remains even in a very smooth geometry. This mode has a longitudinal electrical component and can be easily excited by the beam. By analysing the structure of this mode we have found a way to absorb this mode.

## INTRODUCTION

One of the ways to reach a higher luminosity in colliders is to increase the beam currents. Higher beam currents produce more electromagnetic waves in the Interaction Region (IR) due to the diffraction of the beam fields from the inhomogeneous beam pipe. The structure of the electromagnetic fields excited in an IR is very complicated. Usually each of the colliding beams has a different incoming beam pipe. These beam pipes are combined into one pipe at the collision region. The beams do not generate electromagnetic fields in the smooth part of the beam chamber; however in the interaction region they may generate a lot of electromagnetic waves due to chamber irregularities. Some of the low frequency waves can be trapped in the IR. A trapped mode is characterized by its resonant frequency and the effective shunt impedance. It can happen that the mode resonant frequency is equal to some of the harmonics of the revolution frequency. In this case, the amplitude of the electromagnetic field of this mode will grow until it reaches the value determined by the loaded quality factor together with the loss factor of this mode. The mode loss factor is determined by the interaction of a beam particle with the field of this mode. To interact with a beam particle, the trapped mode must have a longitudinal electrical component, which is collinear with the beam particle velocity. For this reason not all existing Higher Order Modes (HOMs) will interact with a beam particle. Typically, the frequency of HOMs in the interaction region is in the range of several GHz. If some of the HOMs have a large quality factor, of order more than 1000, and the frequency of the mode is in resonance with some harmonic of the revolution frequency, then local heating in the IR can reach tens of kW of power. Other electromagnetic waves, excited by the beam, with a frequency above the cut-off frequency will travel away from IR and go down the beam pipe. The absorption of these waves can bring heating problems in other parts of the accelerator. A large energy loss of the beams in the interaction region can be a severe problem. The temperature of the IR chamber will go up and the vacuum will be spoiled. If the IR chamber has small gaps or hidden cavities (like in shielded bellows or valves), then electric sparks or arcing may cause additional vacuum spikes. Heating of the NEGs (if they are used in the IR) may bring vacuum instability (the temperature can go above the recovery level). All of these things can make the backgrounds much higher. One can find a description of these effects in the publications [1-2].

Detuning (making the mode frequency not equal to any harmonic of the revolution frequency) and the suppression of the loaded quality factor seem to be the only ways to decrease the HOM heating power.

However during the design of the IR we can try to diminish these effects by making the geometry of the IR very smooth and consequently not have so many HOMs. Analysing this problem we found that one mode will still stay in the IR even when the geometry of the metal chamber is very smooth. Of course the reason for this is in the geometry of the connection of two tubes. We will present a description of this mode, which we obtained using two different methods of electromagnetic calculation. One method is by a planar geometry. This method was developed for CSR and wake field simulations [3]. We use this method to make a quick estimate of the power loss, however for a more accurate estimate we did 3D calculations using CST [4] and HFSS [5] codes.

We may note that wake field calculations have been done for IRs of different colliders [6-14]. The IR geometry was mainly determined by the detector setup and shielding of the synchrotron radiation. However the predictions of energy loss in the IR in some publications are many times different and do match experimental measurements [13-14]. In some publications [7] one can find a very small energy loss of order of ten watts, while another publication predicts [12] an enormous power loss of 1 MW in the FCC IR. It is very difficult to imagine that the interaction region can be a highly efficient DC klystron of megawatt power.

## WAVE EXCITATION IN THE IR

Let's start by investigating the reason why we have an additional excitation of the electromagnetic fields in the IR. When a bunch is coming from one connecting pipe

† email address: novo@slac.stanford.edu

*This material is based upon work supported by the U.S. Department of Energy, Office of Science, Office of High Energy Physics, under Contract DE-AC02-76SF00515.*

and passing the junction point where another pipe connects a new electromagnetic field appears in the other connected pipe. At the same time, some part of the bunch field returns back into the other connecting pipe. Fig. 1 shows the electric field line distribution for a time when a relatively long (compared to a pipe diameter) bunch just passed the beam pipe connection.

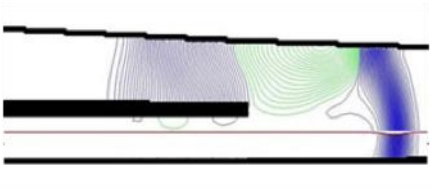

Figure 1: Electric force field line distribution at the time when a relatively long bunch just passed a pipe connection. The red line shows the bunch line charge density distribution and the bunch trajectory.

We can see that the bunch has extended its self-field into the larger common pipe, while some part of the field propagates back into the other pipe and some part is reflected back. This effect is seen more clearly in Fig. 2, where a relatively short (compared to a pipe diameter) bunch passes the pipe connection. We can see that an image charge appears at the edge of the pipe connection. This charge and later the image current (running across the pipes) produces electromagnetic fields in both pipes. This field propagates in time from the edge of the pipe connection. We need to note than a shorter bunch excites more fields in the pipes, due to the excitation of the higher frequency fields, which may freely propagate in the pipe.

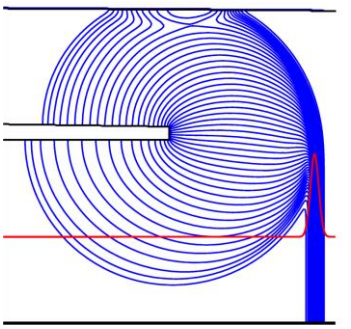

Figure 2: Electric force field line distribution at the time when a relatively short bunch has just passed a pipe connection. The red line shows the bunch line charge density distribution and the bunch trajectory.

In the common central pipe of the IR the electromagnetic fields, which were excited at the edge of the pipe connection chase the bunch. In time the bunch forms a transverse self-field and loses kinetic energy because of this. The self-field is also changing due to the bunch trajectory in the common pipe. The bunch is close to one side near the incoming pipe connection and then goes to the other side of the pipe in order to get into the opposite outgoing pipe. The bunch gets more deceleration as it excites freely propagating electromagnetic fields in this region.

After a bunch has passed the central common pipe region it enters one of the outgoing pipes. Now a newly formed self-field is diffracted at the edge of the pipe connection. Mainly, it is cut by the edge and then propagates into both pipes. The plot of the electric force line distribution for the time when a relatively long bunch has passed the outgoing pipe connection is shown in Fig. 3. We can see also that some part of the field is reflected back into a common central pipe. This field is the source of the HOMs, which will be formed after many reflections. Also there is some part of the field, which continues to chase the bunch.

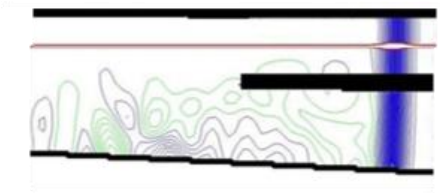

Figure 3: Electric field line distribution for the time when a long bunch has passed the outgoing pipe connection. The red line shows the bunch line charge density distribution and the bunch trajectory.

Electromagnetic fields, excited by a short bunch are more complicated in this region, because there are a lot of fields still chasing the bunch after the pipe connection. Nevertheless among these fields we can see the field from an image charge at the edge of the pipe connection in Fig. 4. We cannot avoid exciting these fields in the interaction region.

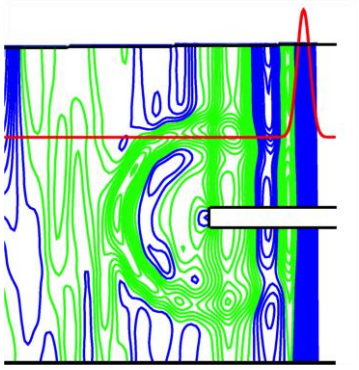

Figure 4: Electromagnetic field line distribution at the time when a short bunch has passed the outgoing pipe connection. The red line shows the bunch line charge density distribution and the bunch trajectory.

## STRUCTURE OF UNAVOIDABLE TRAPPED MODE IN THE IR

In trying to find an optimal geometry for the IR with minimum electromagnetic wave resonance excitation (minimum impedance), we discovered that one mode stays even in a very smooth geometry. First calculations were done using a flat version of the code NOVO for a

flat geometry in the IR. This mode is situated near the connection of the two incoming and outgoing pipes. The electric field distribution and the surface current are shown in Fig. 5 (corresponding left and right plot). The surface charges are concentrated at the edge of the pipe connection and the top and bottom sides of the common central pipe. The surface image currents appear at the time when the image charges start to move to each other. Then the image charges exchange each other. Another image current with opposite sign will change the sign of charges again and oscillations will continue. The frequency of this mode is slightly lower than the cut-off frequency of the common pipe due to the concentration of the electric fields at the edge of pipe connection. Naturally the cut-off frequency of the incoming pipes is much higher than that, of the mode frequency. We therefore have a real trapped mode.

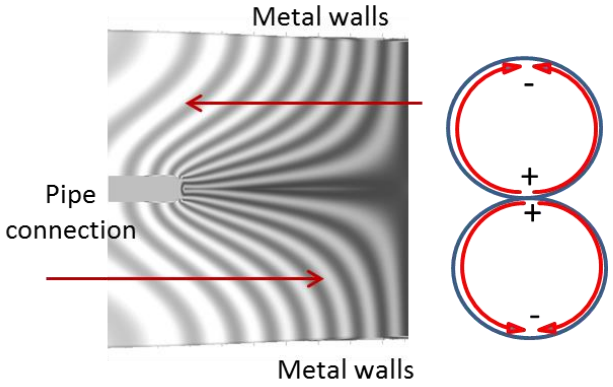


Figure 5: Electric field line distribution (left plot) and surface current distribution (right plot) of the trapped mode. Each surface current plane has a longitudinal slope of the corresponding sign. The red lines show the direction of the colliding beams.

This mode is a combination of a longitudinal and a transverse mode. It can be seen in Fig. 5 that this mode has a longitudinal electric component parallel to the bunch trajectories and can be easily excited by the colliding beams. A bunch produces a stronger interaction with this mode if it travels closer to the pipe connection. The transverse kick from this mode in the incoming pipe connection will be compensated in the outgoing pipe connection (identical to first one) due to the opposite sign of the kick.

## POSSIBLE SMOOTH PIPE CONNECTIONS

In order to diminish the HOM effects we tried to find a geometry for the IR beam pipe that has the smallest impedance. Among other things we considered three different models of the IR all with the same diameter of the incoming pipes and of a central pipe – 30 mm in a diameter:

- *Model 1*: The incoming pipes are smoothly squeezed to a half circle shape in order to merge into the central pipe with a constant diameter.
- *Model 2*: The incoming pipes near the connection are circular pipes. The central part near the pipe connection has a transition to an approximately elliptical or racetrack shape with a double size in the horizontal direction. This connection between the two pipes and the elliptical shape contains some small sharp transitions.
- *Model 3*: Each pipe near the connection has a transition to a half of a special shape determined by the shape of the transition from the central pipe (a proposal from Oide Katsunobu). This is a full smooth geometry.

### *FCC $e^-e^+$ interaction region*

The flexible interaction region design for the future electron-positron circular collider (FCC $e^-e^+$) allows a large beam energy range as the machine will work at different beam energies, from 45.6 GeV up to 175 GeV, with a luminosity that goes from 2.1 × 1036 $cm^{-2}$ $s^{-1}$ for the lower energy to 1.3 × 1034 $cm^{-2}$ $s^{-1}$ for the highest one. The circumference of the machine is foreseen to be about 100 km. The crab-waist collision scheme has been chosen to reach the highest possible luminosity, so the crossing angle is 30 mrad. For the Z-production, to reach a high luminosity it is planned to have a high current of 1.4 A in each beam. Bunches will fill ¾ of a ring circumference. The bunch length will vary from 1.6 mm to 3.8 mm.

All models for the wake field calculations are based on the M. Sullivan design, presented at the FCC week 2017 [15]. The sketch of the IR region is shown below in Fig.7.

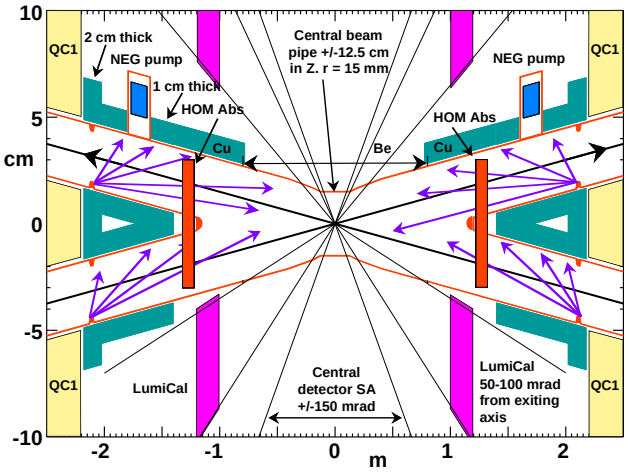


Figure 7: FCC ee IR. The red lines show the boundary of the IR beam chamber.

The IR has a 2.2 m L* and the final focusing magnets are superconductive. SR mask tips are placed at ± 2.1 m, in order to protect the central chamber from photons generated by the last soft magnet whose face is located 100 m from IP. Fig. 7 shows scattered photons (blue arrows)

from these mask tips which become the dominant source of the synchrotron radiation background for the detector.

## *The HOMs analyses*

The wake field or HOMs analyses is based on the calculation of the wake field potential with post processing Fourier analyses. We first find the resonances in the spectrum of the wake field potential. Then we do an eigen-mode calculation in the frequency region around this resonance. In this way we know how much the beam interacts with this mode and the eigen-mode calculation gives us the detailed structure information about this mode. We use the CST code for wake field calculations and we use the CST and HFSS codes for the eigen-mode calculations.

We calculate wake field potentials in a 4 m long part of the interaction region, which includes all important elements. In the calculation we use a Gaussian bunch with 2.5 mm bunch length, however for an initial quick analysis we did calculations for a 10 mm and 5 mm bunch. Initially we designed the geometry of the IR beam pipes using the CST code editor for the geometry. The first and the second model were done in this way. However for a smooth IR geometry we had a problem with the mesh distribution. As this was an important data point we decided to use CAD files as input for the CST and HFSS codes. We got CERN support and professional CAD files. This new approach improves the preparation of the files and, what is important, diminished the problem of the "wild" mesh distribution. The code "CATIA" [16] was used for preparation of the CAD files. We established the file format and additional file description for better communication between "CATIA" and "CST".

## *Model 1: Squeezed incoming pipes.*

The initial calculations were done for the first IR model, which is shown in Fig. 8 [17]. The length of the central beam pipe is 400 mm and the diameter is 30 mm. The cross section near the pipe connection shows how the incoming pipes were squeezed to the half circle shape.

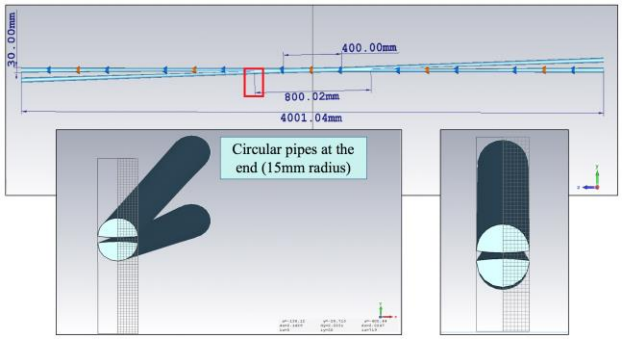


Figure 8: Geometry of the IR Model 1. The cross section near the pipe connection shows how the incoming pipes were squeezed to the half circle shape.

Results of the wake field calculations for this geometry are shown in Fig. 9. The red line in the central plot shows a first 1 m long part of the calculated wake field potential of a 2.5 mm Gaussian bunch. The green line in the central plot shows the bunch linear charge density. The total length of the potential is 2 m. We notice a periodic behaviour of some part the wake field potential. In time this periodic part (a trapped mode) becomes the main part of the potential. Other waves, which have higher frequencies, quickly leave the IR.

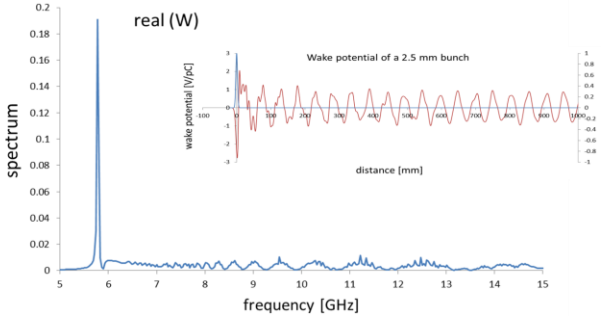


Figure 9: Wake field potential and correspondent spectrum in the IR Model 1.

We calculate the spectrum using the wake field potential of the total length of 2 m. The real part of the spectrum is shown by the blue line in the main plot. The fact that the real part of the spectrum is always positive in the shown frequency range demonstrates the high quality of the calculation of the wake field potential.

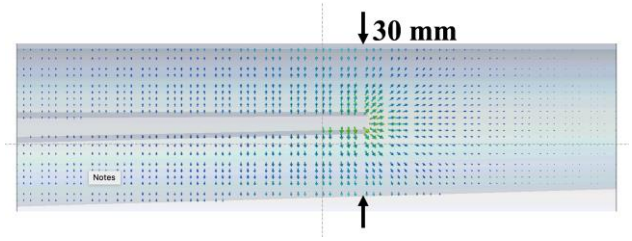


Figure 10: Electric field line distribution for the trapped mode in Model 1.

The spectrum shows only one trapped mode at the frequency of 5.78 GHz. To analyse this mode we performed an eigen-mode calculation in the frequency region of 5-7 GHz and found a resonance mode at 5.774 GHz. This confirms that the beam excites exactly this mode. The electric field line distribution for this trapped mode is show in Fig. 10. We see a similar field distribution as the unavoidable mode, which we discussed before (Fig. 5).

## *Model 2: Small sharp transition.*

The geometry of the second IR model is shown in Fig.11 [17]. In this model the central circular pipe has a transition to an elliptical shape at both sides. The length of each transition is 0.82 m. We performed wake field and spectrum calculations and found only one trapped mode at the frequency of 5.67 GHz. It is interesting that we did see a lower frequency mode because of the larger size of the common pipe. Perhaps a sharp transition destroys the low frequency mode. The real part of the spectrum is shown in the lower right plot of Fig. 11. The structure of

the distribution of the electric field lines is also similar to the unavoidable mode.

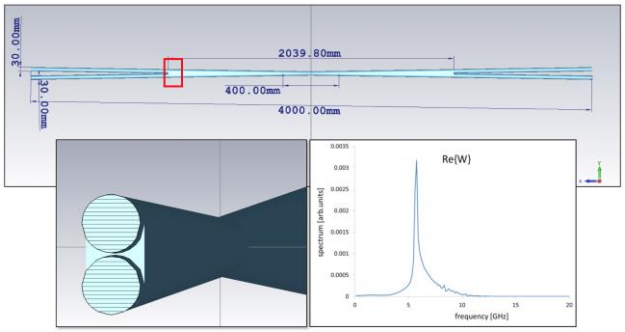


Figure 11: Geometry of the IR Model 2. The cross section near the pipe connection shows two small sharp transitions to the elliptical shape.

### *Model 3: smooth geometry*

The geometry of the third IR mode is shown in Fig.12. In this model the central circular pipe has two transitions on the left and on the right to the some kind of racetrack shape and each incoming pipe also has a transition to half of this shape, so the two pipes together have a cross section of the connecting central pipe.

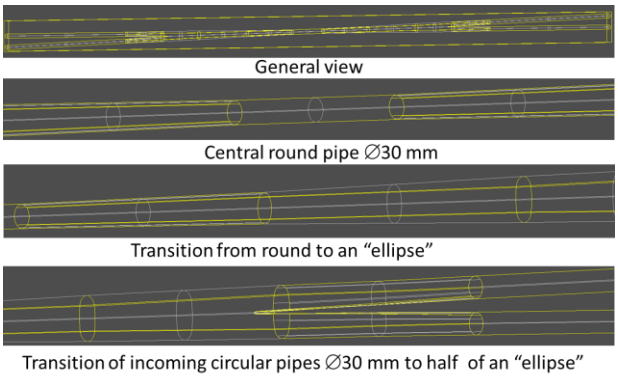


Figure 12: Smooth transition design in IR. Model 3.

Details of the transition of two incoming pipes to a central common pipe can be seen in Fig. 13. This is a very smooth geometry. The central inner part of the pipe connection is rounded to make a smooth edge.

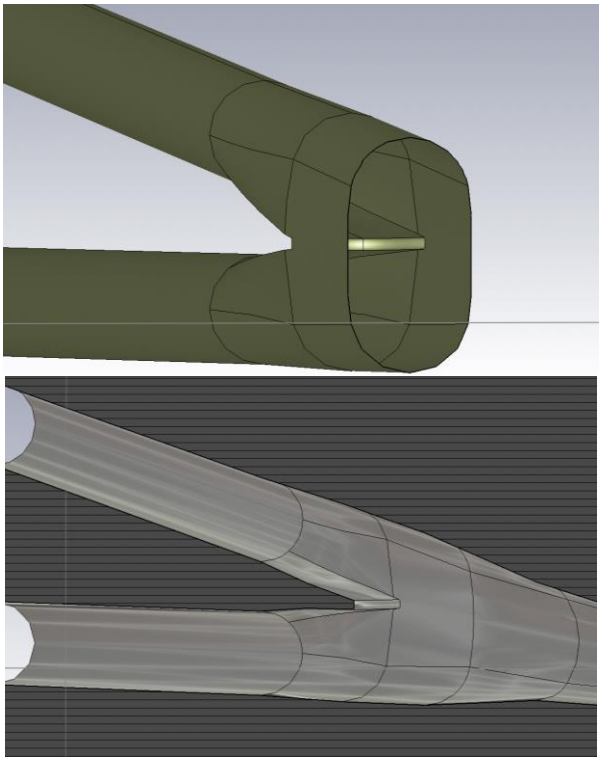

Figure 13: Inside and outside view of the transition in the IR model 3.

The calculated wake field potential of a 2.5 mm bunch in the IR model 3 is shown in Fig.14. Almost all higher frequency modes leave the IR in 2-3 nsec which is just before the arrival of the next bunch. The trapped mode frequency here is almost two times lower than the trapped mode frequency in Model 1. The amplitude is 4 times smaller than the amplitude in Model 1 (Fig. 9). We may conclude that the impedance of the trapped mode in Model 3 is much lower than the impedance of the mode in Model 1.

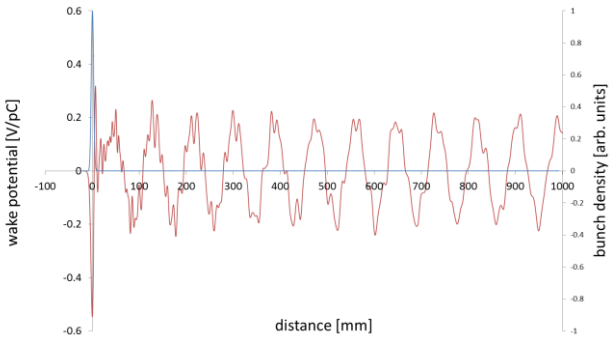


Figure 14: Wake potential (red line) of a 2.5 mm bunch in model 3. The blue line shows bunch linear charge density distribution.

The calculated spectrum (real and imaginary parts) for this model is shown in Fig.15. The frequency of the trapped mode is 3.46 GHz. As we mentioned before, it is lower than the mode found in Model 1 due to the larger size of the common pipe. It is interesting to note the broad-band impedance in the frequency range from 5

GHz to 12 GHz. The amplitude is not very high, but perhaps we need more careful calculations for this frequency range.

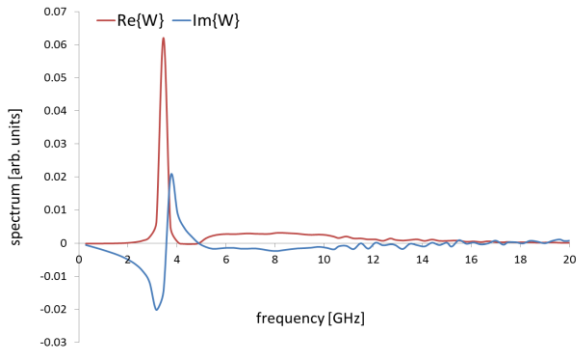


Figure 15: Real and imagery parts of the wake field potential spectrum.

The electric field line distribution of the trapped mode is shown in Fig.16. It is almost identical to the trapped mode in Model 1 (Fig.10) and the unavoidable mode in Fig. 5.

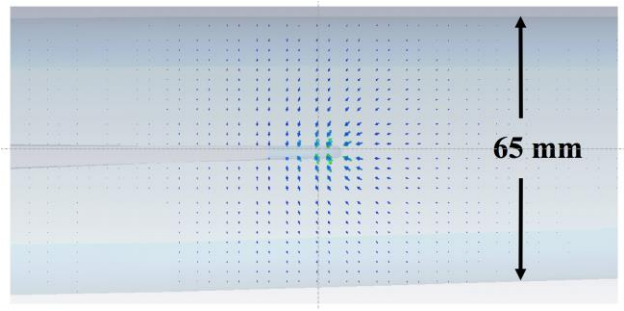


Figure 16: Electric field line distribution for the trapped mode in Model 3.

## HOMS ABSORBER

We now study how to mitigate the effect of the unavoidable mode, which we have found in all three as well as other models. The structure of the mode field distribution shows how we can capture it with a minimum disruption to the image currents of the beam field. The electric field lines in the two incoming pipes are perpendicular to the beam trajectory. We therefore can make longitudinal slots in the top and bottom walls of these pipes (see Fig. 17).

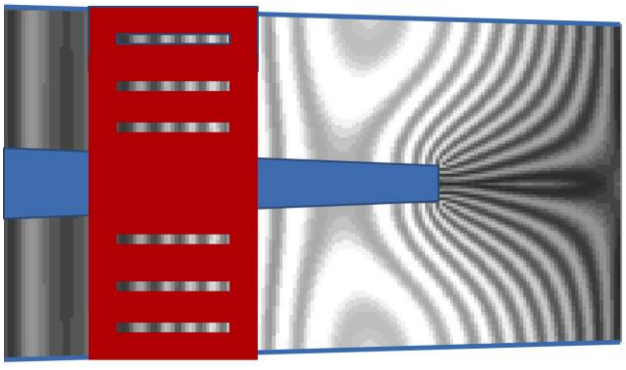

Figure 17: Slots in the top and bottom walls of the incoming pipes.

The slots are oriented perpendicular to the HOM electric field. This allows the mode field to easily propagate though these slots. At the same time, the beam field will not pass through these slots. We can then put a water-cooled absorber above and below the slots. A sketch of the HOM absorber is shown in Fig. 18.

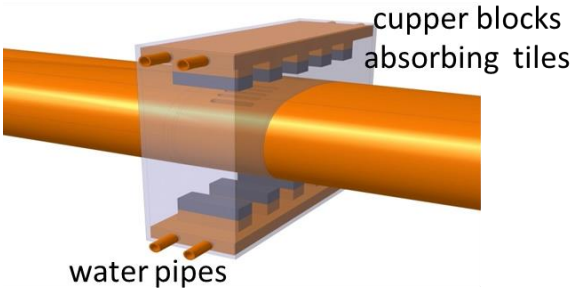


Figure 18: A sketch of a possible HOM absorber.

## CALCULATION OF THE HOM HEATING POWER

To calculate the radiation power we use a cumulative spectral density of the energy losses which is the following integral (details are given in the Appendix)

$$K(\omega) = \mathrm{Re}\{\frac{1}{\pi}\int_0^{\omega} W_s(\omega)\rho(-\omega)d\omega \quad (1)$$

The plot of this integral for Model 3 is show in Fig. 19.

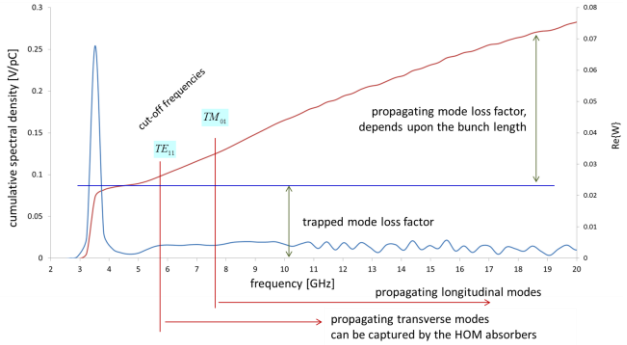


Figure 19: A cumulative spectral density of the energy losses.

The spectral density has a sharp step at the resonant frequency of the trapped mode. The size of this step determines the loss factor of the trapped mode. Cut-off frequencies for $TE_{11}$ and $TM_{01}$ modes (see appendix) are shown by vertical red lines. Above each frequency the transverse fields or longitudinal fields can propagate out of the interaction region. The loss factor of the propagating fields is the part of the density that starts at the cut-off frequency.

Using this plot we can calculate the power loss into the trapped mode using this formula (see appendix)

$$P_{HOM} = 2I^2 k_{HOM}\tau_{l,HOM} \quad (2)$$

where $I$ is the beam current, $k$ is the loss factor of the trapped mode and $\tau$ is the loaded decay time of this mode. The energy loss in the propagating modes is calculated by a similar formula, but now we use a loss factor for the propagating modes and a bunch spacing shown below

$$P_{prop} = I^2 \left(k - k_{HOM}\right) \times \tau_b \qquad (3)$$

We assume that with the water-cooled absorber we can decrease the loaded quality factor of the trapped mode by at least 100. In addition, some fraction of the propagating modes will be captured by the absorber. Estimated numbers for the HOMs heating in the IR with the geometry of Model 1 and Model 3 are shown in the table 1.

Table 1.

| Model # | Trapped mode frequency | Near revolution harmonic numbers | Mode loss factor | Mode decay time | Power of a trapped mode | Propagating modes power | |
|---|---|---|---|---|---|---|---|
| | | | | | | Bunch 5 mm. | Bunch 2.5 mm. |
| | [GHz] | | [V/pC] | [ns] | [kW] | [kW] | [kW] |
| I | 5.774 | 14 &15 | 0.38 | 5.51 | 8.71 | 2.42 | 10.77 |
| III | 3.459 | 8 & 9 | 0.08 | 9.2 | 2.91 | 0.45 | 2.10 |

A sketch of the IR with the geometry of Model 3 together with HOMs absorbers is shown in Fig. 20.

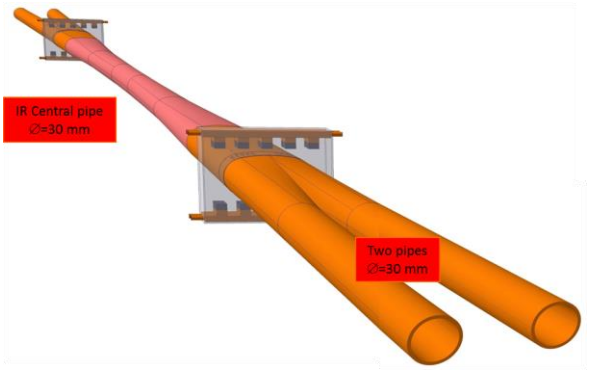


Figure 20: IR smooth geometry with HOMs absorbers

## CONCLUSION

We have designed a smooth geometry of the IR vacuum chamber, which has relatively small HOMs impedance. Each beam of 1.45 A will produce electromagnetic power of approximately 5 KW from both connections. This power will be mainly absorbed in the two sets of HOM absorbers. More work will be needed to further optimize the HOM absorbers.

## ACKNOWLEDGMENT

We would like to thank Frank Zimmerman, Manuela Boscolo and especially Michael Benedikt for their great support of this work. We are also happy to thank Oide Katsunobu, Mauro Migliorati and the MDI team for many useful discussions and help.

Work supported partially by Department of Energy contract DE-AC02-76SF00515.

## APPENDIX

Many formulas in this chapter can be found elsewhere [18-20], however to clarify all the coefficients we repeat several of them.

### *Green's function and wake field potential*

According to the energy conservation law, the power of the excited electromagnetic fields (wake fields) is naturally the power that the beam looses. In order to estimate this power we need to calculate the value of the electromagnetic field that is excited by a charged bunch and that acts back on the single particles of the bunch. Then we can integrate the value of the longitudinal component of this excited electric field $E_z(t,z)$ along the particle's trajectory. This integral which depends upon the longitudinal particle position in the bunch $s$, is called a wake field potential $W(s)$

$$W(s) = \frac{1}{Q}\int_{-\infty}^{\infty} E_z(t,z)_{z=ct-s}\, cdt \qquad (4)$$

The wake potential is usually normalized to the total bunch charge $Q$ and measured in V/pC. Wake fields and correspondent wake potentials can be calculated by integrating Maxwell's equations in the time domain using numerical codes [3-5].

A wake field potential of a point charge can serve as a Green's function $G(s)$ and can be used for calculation of the wake field potentials of the bunches of any line charge density distribution $\rho(s)$

$$W(s) = \frac{1}{Q}\int_{-\infty}^{s} \rho(s')G(s-s')ds' = \frac{1}{Q}\int_{0}^{\infty} \rho(s-s')G(s)ds' \qquad (5)$$

A loss factor $k$, which determines the bunch energy loss, is calculated as an integral of the convolution of the wake potential and the bunch charge density distribution

$$k = \frac{1}{Q}\int_{-\infty}^{\infty} W(s)r(s)\,ds \qquad (6)$$

It has the same dimensions as a wake field potential; however the total bunch energy loss $\Delta\mathcal{E}$ is determined by the loss factor, which is multiplied by the total bunch charge squared

$$\Delta\mathcal{E} = k \cdot Q^2 \qquad (7)$$

### *Frequency spectrum of the wake field potential and cumulative spectral density of energy losses*

Here and later we assume that the particles of the bunch have ultra-relativistic velocities $v \cong c$, where $c$ is the speed of light. The Fourier transform of the wake field potential $W(\omega)$ is defined as an integral

$$W(\omega) = \int_{-\infty}^{\infty} W(s = c\tau)\exp(-i\omega\tau)d\tau \qquad (8)$$

As the wake field potential is a real function then the real part of the transform is a symmetric function of the frequency while the imaginary part is an asymmetrical function of frequency [18].
Using the inverse Fourier transform

$$W(t) = \frac{1}{2\pi}\int_{-\infty}^{\infty} W(\omega)\exp(i\omega\tau)d\omega \quad (9)$$

we can present a loss factor in the following way

$$k = \frac{1}{Q}\int_{-\infty}^{\infty}\rho(s=ct)\left(\frac{1}{2\pi}\int_{-\infty}^{\infty}W(\omega)exp(i\omega t)d\,\omega\right)cdt = \frac{1}{2\pi Q}\int_{-\infty}^{\infty}c\rho(-\omega)W(\omega)d\omega \quad (10)$$

Where $r(w)$ is a Fourier transform of the bunch line charge density distribution

$$\rho(\omega) = \int_{-\infty}^{\infty}\rho(s=c\tau)\exp(-i\omega\tau)d\tau \quad (11)$$

For a single bunch that has a Gaussian shape for the charge density distribution with the RMS bunch length $\sigma$ and the total charge $Q_b$ the Fourier transform is

$$\rho(\omega) = \frac{1}{c}Q_b e^{-\frac{1}{2}(\omega\frac{\sigma}{c})^2} \quad (12)$$

If the spectrum of the bunch density distribution has only a real part (like a Gaussian distribution) then we need only the real part of the spectrum of the wake field potential.

Based on (7) and changing the upper limit of the integral to a finite value, we will introduce a Cumulative Spectral Density of the energy losses

$$k(\omega) = \frac{1}{\pi}\int_0^{\omega} c\rho(\omega)\,\mathrm{Re}\{W(\omega)\}d\omega \quad (13)$$

Cumulative spectral density of the energy losses is shown in Fig. 5. We can see a sharp step near the resonance. We can calculate the intrinsic impedance $R/Q$ of this resonance using the following formula, where $\Delta k$ is the size of this step (loss factor of this mode):

$$R/Q = 2\frac{\Delta k}{\omega}\text{、} \quad (14)$$

The frequency spectrum of the wake field potential shows us if any resonance exists in the low frequency range. It may reflect the fact that low frequency modes may be trapped in some kind of cavity and oscillate there for some time. Actually this time is determined by the loaded quality factor of this mode. These electromagnetic fields after a time of several oscillations will leak out of the cavity and propagate down the beam pipe. For this reason in the high frequency range the spectrum is a more or less smooth function of the frequency. We may assume that the frequency which separates different spectrum behavior is the cut-off frequency.

## *Cut-off frequencies*

Usually we consider some geometry (like a cavity), which is different to the geometry of the incoming and outgoing pipes. In our case this is the connection of two beam pipes. The cut-off frequency is the minimum frequency of the electromagnetic wave, which may propagate in the incoming and outgoing pipes. Below this frequency the field can be trapped in the "cavity". The cut-off frequency is determined by the geometry of the beam pipe. There can be several types of propagating waves like transverse magnetic (TM) or transverse electric (TE). For a round beam pipe of radius $a$ the minimum cut-off frequency is the frequency of the longitudinal TM01 mode

$$f_{TM_{01}}^{cut-off} = \frac{c}{a}\times\frac{\nu_{01}}{2\pi};\quad \nu_{01} = 2.4048 \quad (15)$$

In our calculations the radius of the beam pipe is 15 mm that corresponds to a cut-off frequency of 7.65 GHz. However a transverse mode TE11 has a lower cut-off frequency

$$f_{TE_{11}}^{cut-off} = \frac{c}{a}\times\frac{\mu_{11}}{2\pi};\quad \mu_{11} = 1.8412 \quad (16)$$

In our case it is 5.86 GHz. This mode has a transverse electric component and may propagate through the longitudinal slots, or between the fingers of shielded elements like bellows and valves. A plot of the cumulative spectral density of energy loss (Fig. 19) will give us information on how much energy a bunch loses for modes below or above the cut-off frequency.

## *Power loss of a train of bunches below and above cut-off frequency*

According to [19] the beam power loss due to the resonant excitation of a trapped mode is

$$P_n = I^2\left(R/Q\right)_n Q_l f(\tau_l,\tau_b)$$
$$f(\tau_l,\tau_b) = \frac{\tau_b/\tau_l\left[1-\exp\left(-2\tau_b/\tau_l\right)\right]}{2\left[1-2\exp\left(-\tau_b/\tau_l\right)\cos(\Delta\omega)\tau_b+\exp\left(-2\tau_b/\tau_l\right)\right]} \quad (17)$$

In the case where the decay time of this mode $\tau_l = 2Q_l/\omega$ is much longer than the bunch spacing $\tau_b$, we can write the following

$$P_n = 2k_n I^2\tau_l \quad (18)$$

In the opposite case where the mode decays before the arrival of the next bunch, the power loss is

$$P_n = k_n I^2\tau_b \quad (19)$$

## REFERENCES


[1] A. Novokhatski, J. Seeman and M. Sullivan, "Analysis of the wake field effects in the PEP-II storage rings with extremely high currents," *Nucl. Instr. Meth.*, vol. A 735, pp.349–365, 2014.

[2] A. Novokhatski, J. Seeman, M. Sullivan and U. Wienands, "Electromagnetic waves excitation, propagation and absorption in the high current storage rings*", IEEE Trans.on Nucl.Sci*, vol. 63, no 2, pp.812-817, 2016

[3] A. Novokhatski, “Field dynamics of coherent synchrotron radiation using a direct numerical solution of Maxwell’s equations”, *Phys. Rev. ST Accel. Beams*, vol. 14, p. 060707, 2011.

[4] The MAFIA collaboration “User Guide”, CST GmbH, Darmstadt, Germany

[5] HFSS. http://www.ansys.com/products/electronics/ansys-hfss

[6] S. Weathersby and A. Novokhatski, “Wake fields in the Super B factory interaction region”, in *Proc. 1st Int. Particle Accelerator Conf. (IPAC’10)*, Kyoto, Japan, May 2010, paper TUPD026, pp. 2105-2107

[7] A. Novokhatski and M. Sullivan, “Beam fields and energy dissipation inside the Be beam pipe of the Super-B detector”, in *Proc. 1st Int. Particle Accelerator Conf. (IPAC’10)*, Kyoto, Japan, May 2010, paper TUPEB081, pp. 1578-1580

[8] K. Shibata and K. Kanazawa, “Loss factor and impedance of IR beam duct for Super-KEKB and KEKB”, in *Proc. 1st Int. Particle Accelerator Conf. (IPAC’10)*, Kyoto, Japan, May 2010, paper TUPD042, pp. .

[9] R. Wanzenberg *et al.*, “Calculations of Wakefields for the New Design of the LHCb Vertex Locator”, CERN, Geneva, Switzerland, CERN-ACC-NOTE-2017-0034, May 2017.

[10] R. Wanzenberg *et al.*, “Calculation of Wakefields and Higher Order Modes for the Vacuum Chamber of the ATLAS Experiment for the HL-LHC”, CERN, Geneva, Switzerland, CERN-ACC-NOTE-2013-0046, Dec 2013.

[11] A. Novokhatski, “Wake potentials in the ILC Interaction Region”, Proc. of the 2011 Particle Accelerator Conference, New York, NY, USA, 2011, pp.1837-1839

[12] G. Stupakov, “Estimates of local heating due to trapped modes in vacuum chamber,” MDI Meeting, CERN, Geneva, Switzerland, April 2016.

[13] A. Novokhatski, “Overall HOM measurement at the high beam currents in the PEP-II SLAC B-factory”, in *Proc. Particle Accelerator Conf. (PAC’07)*, Proceedings of PAC07, Albuquerque, New Mexico, USA, June 2007, paper MOOAKI02, pp. 45-47

[14] A. Novokhatski , S.DeBarger, S. Ecklund, N.Kurita, J.Seeman, M.Sullivan, S.Weathersby, U.Wienands, “A new Q-2 Bellows absorber for the PEP-II SLAC B-factory”, in Proc. Particle Accelerator Conf. (PAC’07), Proceedings of PAC07, Albuquerque, New Mexico, USA, June 2007, paper FRPMS076, pp. 4219-4221.

[15] FCC week 2017, 29 May-2 June 2017, Berlin, Germany.

[16] CATIA, ***http://www.catia.com.pl/***

[17] E. Belli, “Trapped mode analysis” , FCC-ee MDI workshop, 16-27 January 2017, CERN, Geneve, Switzerland, ***https://indico.cern.ch/event/596695/***

[18] B. Zotter and S. Kheifets “Impedances and Wakes in High Energy Particle Accelerators”, World Scientific Publishers (1998).

[19] L. Merminga et al., “Specifying HOM-power extraction efficiency in a high average current, short bunch length SRF environment”, Proceeding of the XX International Linac Conference, Monterey, p.860 (2000).

[20] A.Novokhatski, “HOM calculations of new RF cavities for super B-factory”, Proc. of the Super B Factory Workshop in Hawaii. January 19-22, 2004, Honolulu, SLAC–PUB–10792, October 2004.